Fladis field experiments. Final report

Nielsen, M.; Ott, Søren

Publication date:
1996

Document Version
Publisher's PDF, also known as Version of record

Risø–R–898(EN)

Fladis Field Experiments Final Report

Morten Nielsen and Søren Ott

Risø National Laboratory, Roskilde, Denmark
July 1996

Abstract The objective of the Fladis £eld experiments was to investigate dispersion of lique£ed ammonia with equal attention to the near-source aerosol jet, the intermediate heavy gas dispersion phase, and the downstream transition to passive dispersion. The present report presents the sensor layout and gives an overview of the available experimental data. The average concentration £eld is parametrized by Gaussian distributions. This is done for observations in a £xed frame of reference and relative to the instantaneous plume centre line. The moving frame statistics are expected to compare better with wind tunnel simulations and numerical models which do not include plume meandering. The plume mass ¤ux is estimated from the observed plume pro£les and compared to the release rate. Average surface concentrations are found with a special interpolation method, and this is used to study how the averaging period affects the plume footprint. The instantaneous plume is non-Gaussian, and this is demonstrated by Lidar measurements in the far £eld and thermocouple measurements in the near-source jet. Probability functions and a spatial correlation for the concentration are found. The heat budget of the plume shows signs of heat ¤ux from the ground. The composition of the liquid aerosols was observed to change from almost pure ammonia to almost pure water.

A new two-dimensional 'shallow layer' type model SLAM is developed, and an existing 'box' type model for heavy-gas dispersion on a uniform terrain is generalized.

Contracts No. EV5V–CT92–0069 (CEC)
D5226–92–11821 (NUTEK)

The project was funded by the ENVIRONMENT Programme under D.G. XII of the Commission of the European Communities in collaboration with NUTEK (S).

ISBN 87–550–2184–0
ISSN 0106–2840

Information Service Department · Risø · 2002

Contents

Summary

This report documents the CEC ENVIRONMENT project called FLADIS FIELD EXPERIMENTS, and it may be summarized by the following main points:

- The £eld experiment project was linked to the main Fladis project[1] but delayed in time. *main Fladis project*
- Three £eld campaigns with a total of 27 trials were conducted. Data from 16 of these trials were prepared for distribution, and the desired combination of long release durations and favourable wind conditions was obtained in about 6 cases. We managed to transfer information from at least one good experiment to users in the main project. *trials*
- The gas source was a horizontal downwind jet of lique£ed ammonia with release rates of 0.25–0.5 kg/s and release durations up to 40 minutes. *release type*
- The release conditions for the available experiments are listed in a table. This includes estimates of the jet ¤ow force and molar weight appropriate for isothermal wind tunnel simulations. *release conditions*
- The release rates were checked against the weight of the released amount of ammonia. The plume mass ¤ux was estimated by £eld observations and found to be within 16% of the release rate. *release rate*
- The ammonia was detected by horizontal chains of sensors across the plume from near the source to the stage of passive dispersion. This sensor layout was optimized for detection of the plume width and centre-line position. *sensor array*
- Gaussian pro£les were £tted to average concentrations from the horizontal chains of sensors — both in a £xed frame of reference and relative to the instantaneous plume centreline. The vertical pro£les were of an exponential shape. The average plume pro£les may be used as a reduced data set for a preliminary data analysis. *mean concentration £eld*
- Plume meandering is less dominant in a wind tunnel than in the £eld, and it is usually non-existent in numerical models. Therefore, moving frame statistics are often more appropriate for model evaluation than £xed frame statistics. From a risk analysis point of view, it may be more relevant to know typical plume concentrations than the average of a meandering plume. Finally, our moving frame curve £ts are more accurate, since these pro£les usually were more Gaussian. *advantages of moving frame statistics*
- An interpolation method to determine the average surface concentration or plume footprint was developed. Due to plume meandering the plume footprint widens with increasing averaging times. The footprint area was insensitive to average time. *plume footprint*
- Concentration ¤uctuations were measured by fast gas detectors. The concentration ¤uctuations followed the power law typical for an inertial subrange. The probability distribution of the fast signals depends on the distance from the core of the plume. The spatial correlation of concentration ¤uctuations followed the function $\propto \exp\{-\delta y^{2/3}\}$, in which δy is the cross-plume horizontal separation. *concentration ¤uctuations*
- A remote sensing Lidar detected instantaneous concentration pro£les along a laser beam which was directed horizontally across the plume. Point samples of these agreed with signals from nearby fast concentration sensors. The instantaneous pro£les were far from Gaussian and the gas traces were sometimes broken by sudden changes of the wind direction. *instantaneous concentration pro£les*

- The enthalpy content was estimated from adjacent measurements of temperature and concentration. The enthalpy in the £eld was compared to that of the source and the mixing was found to be not perfectly adiabatic. This indicates a heat ¤ux from the ground which reduces the density difference relative to the ambient by O(20%). *enthalpy budget*

- The composition of the aerosols in the two-phase jet changed from almost pure ammonia to almost pure water within a few meters. This supports the hypothesis of homogeneous thermal equilibrium. *aerosol composition*

- The data were distributed with documentation £les and a set of utility programs. The utilities makes it possible to inspect time series, watch computer animations of wind and concentration £elds, calculate average pro£les, £nd probability density functions, and export time series to an easy-to-read £le format. Precalculated block statistics may be imported by commercial spreadsheet programs, for a quick data analysis. The utility programs were integrated in a user-friendly program shell. *data distribution with utility software*

- A new shallow layer model SLAM was developed. SLAM has the following distinct features compared to other shallow layer models: *new shallow layer model*

  – The turbulent kinetic energy budget is explicitly accounted for.

  – The entrainment rate is estimated on the basis of local turbulent kinetic energy.

  – The vertical pressure is not assumed to be hydrostatic.

  – A Lagrangian grid is used in the numerical solutions.

  – Numerical methods ensure that conservation laws are not jeopardized even for coarse grids.

  The model was calibrated with the instantaneous heavy-gas release in Thorney Island trial 8. This is a challenging reference case which has an accelerating cloud, a dominant slumping process, and strong strati£cation.

[1]The full name of FLADIS is: *Research on the dispersion of two-phase ¤ashing releases*.

1 Introduction

background

The Fladis project followed the MTH project BA, reported by Builtjes (1992). Project BA involved a propane dispersion experiment which focused on the in¤uence of obstacles on heavy gas dispersion (see Heinrich & Scherwinski 1990, Nielsen & Jensen 1991). When planning of the Fladis project we decided to follow an initial heavy gas plume to the stage of passive dispersion.

motivation

The interest in this problem was motivated by the hazards of toxic lique£ed gases, which may still be harmful at relatively weak concentrations. We had two reasons to choose ammonia as a released substance. First, the use of ammonia is increasing in industry, e.g. as an alternative cooling agent substituting freon and as a compound used in smoke denitri£cation units at fossil fuel power plants. Secondly, the density of an ammonia cloud is a challenge to heavy-gas dispersion models, because it is especially sensitive to air moisture and heat input from the ground. The molar weight of ammonia is lighter than that of air, and an ammonia plume can only be heavy due to the temperature de£cit caused by initial evaporation. Heat transfer from the surroundings and heat from reaction with air moisture modify the density difference.

other ammonia experiments

The most wellknown lique£ed ammonia dispersion experiments are the Desert Tortoise series of Goldwire, McRae, Johnson, Hipple, Koopman, McClure, Morris & Cederwall (1985). The release rates in Desert Tortoise were much higher than in the present experiments, and the dispersion was therefore more affected by gravity. In the Desert Tortoise experiments a pool of liquid ammonia formed in front of the release point, but due to differences in the release systems[2], this did not happen in the present experiments. Other differences are the lower ambient temperature and the higher air humidity in Fladis, which is more representative for a European climate. Generally, the release durations were longer than in Desert Tortoise. We are aware of two additional heavy gas experiments with ammonia (Resplandy 1969, Pfenning, Millsap & Johnson 1987), but the instrumentation of these was modest compared to that of Desert Tortoise and Fladis. New large-scale ammonia £eld experiments, focusing on liquid rain-out after jet impingement, are planned in 1997–1998 by Institute National de lÁEnvironment Industriel et des Risques, France.

[2] a nozzle contraction provided a higher exit pressure in the present experiments

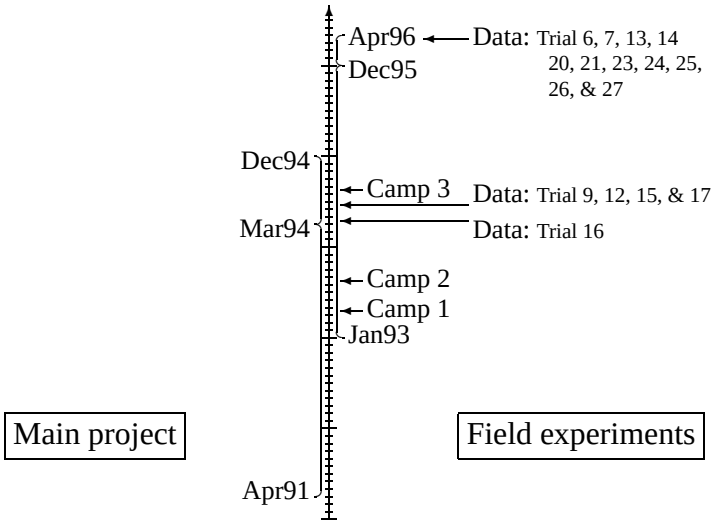

Figure 1. Timing of the Fladis £eld experiments in relation to the main Fladis project.

1.1 Project development

link to the main Fladis project

The £eld experiments were originally planned as part of the main Fladis project, supported by the CEC contract STEP–CT91–0125 and reported by Duijm (1994). Unfortunately, the important contribution proposed by TüV Norddeuchland was withdrawn due to lack of additional funding, but the remaining participants in the £eld work, Risø and FOA, decided to reconstruct the £eld experiment part of Fladis. A new test site was found at the training facilities of Hydro-Care in Landskrona, Sweden. This was a convenient solution, since Hydro-Care already had a permission for ammonia releases and a full safety organization. CBDE was invited to contribute with measurements by a newly developed very fast responding concentration sensor. Finally, CERC joined the project in order to strengthen the theoretical aspects of the work.

time schedule

The £rst £eld campaign was conducted four months after contract signature, and the second campaign involving the complete instrumental setup took place after eight months. The start of the project was a busy period during which we constructed the release system, built terminal boxes for data acquisition, enhanced data acquisition software, and bought pressure transducers, concentration sensors, and meteorological equipment.

Time was of major concern because the £eld experiments were much delayed relative to the main Fladis project as sketched in £gure 1. The critical milestone was the data transfer which ought to leave suf£cient time for data analysis and reporting within the main project. The following actions were taken to minimize the effect of the delay:

- The main Fladis project was extended by 9 months.
- The data transfer was split into several packages.
- The data were preprocessed and distributed with software which eased the work of the analysts.
- The data analysts made more use of the previous propane trials.

Most data users in the main Fladis concentrated on trial 16, which at the conclusion of the second £eld campaign was the most successful one. In order to give priority to data transfer and documentation of the available results, the third measurering campaign was postponed relative to the original plan. This implied that data from the last £eld campaign became too late for the main Fladis project, but we did our own analysis in (Nielsen 1996b) and (Nielsen, Ott, Jørgensen, Bengtsson, Nyrén, Winter, Ride & Jones 1997).

1.2 Project organization

The project involved three aspects: £eld experiments, data analysis, and numerical work. The £eld activities were interdependent, and the four partners, Risø, Hydro-Care, FOA and CBDE, worked close together during the experimental phase of the project in the £rst half of the project. In order to enhance the data quality, FOA and CBDE processed time series from their own instruments, and the processed data were sent to Risø who assembled a joint and synchronized data base.

The formulation of a new ‘shallow water’ type numerical model at the System Analysis Department of Risø was an independent activity. According to the original plan CERC were to enhance a similar existing model and provide some liason between the main Fladis project and the Fladis Field project. However, it proved inappropiate to enhance the existing model and, with the agreement of the CEC, more effort was placed on analytical studies of the gas source.

role of participants

The role of the participants may be described by the following key words:

Risø Coordination, experimental planning, meteorological, temperature, and Lidar measurements, arti£cial smoke, data acquisition, data processing, data distribution, data analysis, and numerical modelling.

Hydro-Care Test facility, construction of the release system, ammonia supply, safety organization, safety equipment, reference mast, and concentration measurements.

FOA Design of the release system and source measurements.

CBDE Measurements of concentration ¤uctuations and processing of these data.

CERC Numerical modelling and analysis.

Addresses of the project partners and names of contact persons are given in appendix C.

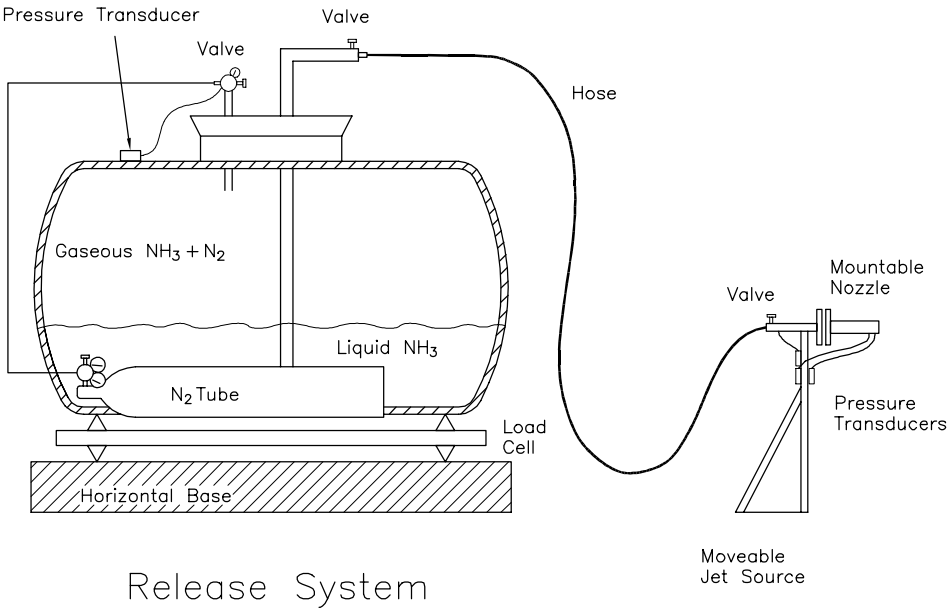

Figure 2. The release system consisted of a pressurized liquid ammonia tank connected to a movable source with mountable nozzles. The system was monitored by pressure transducers and by temperature probes in the nozzle and on the side of the tank.

2 Field experiments

2.1 Experimental design

release system

Figure 2 shows the release system. The ammonia was extracted from the liquid phase of an industrial standard tank, which was pressurized by nitrogen. In order to avoid ¤ow distortion, the source was moved away from the tank and connected with a hose. Mountable release nozzles were designed with a smooth contraction followed by a thin channel to the outlet. The friction of the accelerated ¤ow through the outlet channel was associated with a pressure drop, which assured that the ammonia was always in the liquid phase at the contraction. With this design the ¤ow rate could be calculated suf£ciently accurate by the measured pressure drop in the nozzle contraction. A third pressure measurement near the outlet enabled an estimate of the jet ¤ow force, using the method of Nyrén & Winter (1987). These measurements were made by ceramic pressure transducers (Valcom). The tank and nitrogen supply were put on a load cell (Toledo) for an independent check of the ¤ow rate. The average disagreement between the calculated emission and the weight loss of the ammonia tank was found to be 2% for the medium size nozzle and 5% for the largest nozzle. This was an important improvement from the questioned release rates in the previous propane experiments (Nyrén & Winter 1990).

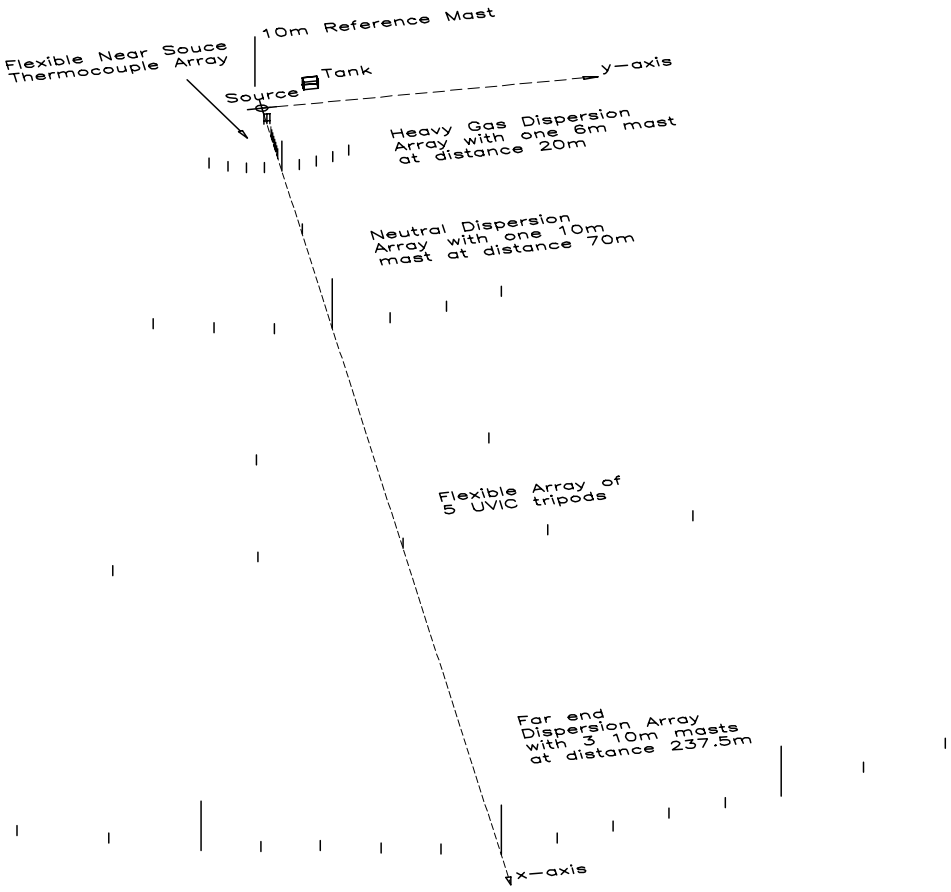

Figure 3. Default experimental setup during the second and third £eld campaign.

sensor layout

Figure 3 is a sketch of the sensor array. Most of the concentration sensors were arranged in three arcs across the expected plume at 20, 70, and 238 m distance. The horizontal separation of the instruments increased from 3 m in the £rst arc to 10 m in the last one. About 5 instruments were simultaneously exposed in each measurering chain. In order to detect the variable plume position and make use of more wind directions, the measurering array was made wider than the instantaneous plume width. The £rst measurering arc had sensors at two levels whereas the other ones have sensors at one level only. The vertical concentration pro£le was measured by instruments on 10-m masts at the array centre line and at two additional positions int the sensor array at 238-m distance.

concentration sensors

The operational principle of the concentration sensors placed in the area up to 70 m from the source was a catalytic combustion (Dräger Ex). The concentration £eld in the last arc of sensors was detected by instruments with electrochemical cells (Dräger NH_3). The fast responding concentration sensor of CBDE (Uvic®) applies a method of ionization by ultra-violet light, and these instruments were mounted either on the centre-line masts at 238-m distance or on movable tripods. The centre-line mast at 20-m distance carried sonic anemometers (Kaijo Denki) with attached thermocouples. The difference between the distorted sound virtual sonic temperature and the true temperature of the thermocouple was used to detect relatively fast concentration ¤uctuations. This technique was developed in the previous propane experiments (Nielsen, Jensen & Ott 1990).

Lidar

The operational principle of the Risø Lidar is to £re a short pulse of laser light and detect the backscatter from airborne particles. Due to differences in the time-of-¤ight, the re¤ected light becomes a transient signal which is transformed into the spatial particle concentration along the laser beam. The measurering is instantaneous compared to the dispersion process and the spatial resolution is ≈ 1.2 m. A presentation of the Li-

dar system and its application in other dispersion experiments is found in Jørgensen & Mikkelsen (1993). In Fladis the Lidar was deployed 220 m downstream of the source where normally the pure ammonia plume would be invisible. An arti£cial smoke was therefore added to the ammonia plume in these trials. The mass of the added smoke was ≈2% of the released amount of ammonia.

other instruments

The reference mast upstream of the release point carried instruments to measure the ambient wind pro£le (Risø cup anemometers), wind direction (Risø wind vane), turbulence (Solent ultra-sonic anemometer), humidity (Frankenberger psycrometer and Vaisala solid state sensor), and solar radiation (Kipp & Zonen pyranometer). The atmospheric pressure was messured by a barometer (Vaisala) inside a cabin. The temperature de£cit of the ammonia jet was detected by thermocouples arranged in different combinations in an area up to 20 m from the source. A thermocouple was also placed next to each concentration sensor in the array at 20-m distance. The centre-line mast at 20-m distance was equipped with similar thermocouples and concentration sensors plus instruments for detection of humidity (Vaisala), short-wave radiation (Kipp & Zonen albedometer), long-wave radiation (Kipp & Zonen pyrgeometer) and surface temperature (Hiemann thermometer). The 10-m masts further downstream were equipped with instruments to measure wind speed, wind direction, air humidity, and atmospheric turbulence.

Table 1. Instrument distribution with downwind distance.

Measurement	**Instrument type**	**Number of instruments**					
		-7m	0m	10m	20m	70m	238m
Pressure	Transducer		4				
Tank weight	Load cell		1				
Concentration	Catalytic				22	12	
	Electrochemical						22
	Uvic®						10[a]
	Sonic anemometer[b]				3		
	Lidar[c]						1[d]
Temperature	Thermocouple		2	64[a]	29		
Speed	Cup anemometer	3				3	5
Direction	Wind vane	1				1	2
Turbulence	Sonic anemometer	1				1	1
Humidity	Psycrometer	1					
Hum. & temp.	Solid state w. Pt100	1			1	2	
Short-wave rad.	Pyranometer	1					
	Albedometer[e]				1		
Long-wave rad.	Pyrgeometer				1		
Surface temp.	Infrared[f]				1		
Air pressure	Barometer[g]	1					

[a] sometimes rearranged
[b] equipped with thermocouple
[c] beam across the plume
[d] only trial 23 & 25
[e] upward and downward pyranometer
[f] remote sensing
[g] solid state sensor

overview

Table 1 provides an overview of the instrumentation. Further details on data acquisition, signal processing, and instruments are reported in Nielsen, Bengtsson, Jones, Nyrén, Ott & Ride (1994).

Table 2. Overview of release conditions. All parameters are calculated over the release period of each trial and the standard deviations of wind speed and direction are therefore not directly comparable. The wind direction is measured at 10-m height, except in trials 6 and 7 (campaign 1) where it has been measured at the 4 m level.

Trial	Date	Time	⌀	∠	p_0	T_0	ṁ	F_{jet}	M_{eff}	T_{dur}	u_{10}	Δ_{Dir}	σ_u	σ_{Dir}	u_*	L	p_{air}	T_{air}	R.H.	$I_{\downarrow}$
6	7/4/93	13:25	6.3	→	5.9	7	0.42	24	92	10	2.7	2	0.64	18.5	0.36	-51	—	9	67	—
7	7/4/93	14:00	6.3	→	5.7	7	0.42	24	92	5	2.9	4	0.62	18.7	0.34	-28	—	8	57	—
9	7/8/93	14:39	6.3	→	6.9	14	0.40	27	89	15	6.1	5	1.35	12.3	0.44	348	1020	16	86	131
12	10/8/93	15:31	4.0	↑	7.2	16	0.20	13	88	5	2.2	-7	0.57	14.2	0.15	-61	999	16	75	247
13	11/8/93	14:25	6.3	→	7.7	18	0.50	34	87	15	5.5	-27	1.03	9.5	0.48	-164	1008	16	52	653
14	11/8/93	15:51	6.3	→	7.4	17	0.47	32	88	10	5.2	-31	1.15	11.7	0.45	-174	1008	17	53	509
15	13/8/93	19:18	6.3	→	7.7	18	0.51	34	87	3	5.9	-7	0.91	8.0	0.50	271	1019	17	60	134
16	13/8/93	19:51	4.0	→	8.0	17	0.27	18	88	20	4.4	-8	0.87	9.6	0.41	138	1020	16	62	85
17	13/8/93	21:09	4.0	→	7.9	15	0.27	18	88	25	3.7	-28	0.72	9.6	0.31	59	1020	16	63	0
20	23/8/94	12:29	4.0	→	7.9	16	0.23	15	88	40	4.0	-7	0.70	12.8	0.38	-25	1018	20	69	660
21	23/8/94	16:50	6.3	→	6.5	12	0.57	29	89	40	4.3	24	0.78	10.0	0.34	-53	1017	21	59	390
23	30/8/94	11:56	6.3	→	7.6	16	0.43	28	88	20	6.6	-7	1.24	9.5	0.53	-112	1012	17	54	674
24	30/8/94	16:06	6.3	→	5.7	9	0.46	18	90	10	4.9	-6	0.84	9.7	0.41	-77	1013	18	54	448
25	30/8/94	16:38	6.3	→	5.9	9	0.46	21	90	22	4.5	-6	0.87	11.8	0.43	-201	1013	17	54	239
26	31/8/94	14:49	4.0	→	8.3	20	0.21	12	86	10	3.0	-31	0.48	13.6	0.29	-16	1019	19	52	606
27	31/8/94	16:41	4.0	→	8.5	20	0.22	13	86	21	2.4	-10	0.51	19.6	0.25	-22	1019	19	50	326

Headings:

Time	Start of release	M_{eff}	'Effective' molar weight [g/mole]
⌀	Nozzle diameter [mm]	T_{dur}	Release duration [min]
∠	Jet direction	u_{10}	Average wind speed at 10 m [m/s]
p_0	Exit pressure [Bar]	Δ_{Dir}	Wind direction relative to ideal [Deg]
T_0	Nozzle temperature [°C]	σ_u	Standard deviation of wind speed [m/s]
ṁ	Release rate [kg/s]	σ_{Dir}	Standard deviation of wind direction [Deg]
F_{jet}	Jet ¤ow force [N]	u_*	Friction velocity [m/s]
L	Monin-Obukhov length [m]		
P_{air}	Atmospheric pressure [mBar]		
T_{air}	Ambient temperature [°C]		
R.H.	Relative humidity [%]		
$I_{\downarrow}$	Insolation [W/m^2]		

2.2 Release conditions

Table 2 provides an overview of the trials which are suitable for analysis. All parameters in this table are averaged over the individual release period.

The exit pressure p_0 is measured at the outlet whereas T_0 is the temperature measured *release parameters*

upstream of the nozzle contraction. The release rate $\dot{m}$ is calculated from the pressure drop through the conical nozzle contraction. The jet ¤ow force F_{jet} is evaluated from the release rate and the pressure, temperature, and an estimate of the vapour fraction at the exit. The 'effective' molar weight M_{eff} is a concept de£ned in Nielsen & Ott (1995). It was introduced because scaling laws of heavy gas dynamics, as de£ned in (Britter & McQuaid 1988) or (König-Langlo & Schatzmann 1991), characterize the heavy gas effect by the relative density difference between gas and ambient air $(\rho/\rho_{\mathrm{air}} - 1)$, which in many cases is $= (M/M_{\mathrm{air}} - 1)$. This relation is, however, only true if the gas release is isothermal as common in wind-tunnel experiments. If the dilution process is adiabatic and all aerosols have evaporated, the scaling laws may be applied with the isothermal model gas which have the 'effective' molar weight M_{eff}.

meteorology

The wind speed u_{10} and the wind direction relative to the preferred one Δ_{Dir} are average values of measurements from four locations in the £eld. Their standard deviations σ_u and σ_{Dir} are calculated as the mean of the local standard deviations, i.e. the contribution from spatial variation of the mean values is not included. The friction velocity u_* and the Monin-Obukhov length L are based on measurements by the sonic anemometer at the 4 m level of the upstream reference mast. The ambient temperature T_a, the relative humidity R.H., and the short-wave downward radiation $I_{\downarrow}$ are measured at the 1.5 m level.

trial evaluation

The information in the table should contain suf£cient input for most heavy-gas dispersion models. Trial 16, 20, 23, 24, 25, and 27 are probably the best ones for model comparison, since these had long release duration and favourable wind directions. The wind direction of trial 9 had a £ne average but a distinct trend, moving the plume from one side of the array to the other one. Trial 6 was done under favourable atmospheric conditions, but it should be remembered that the instrumentation was limited during the £rst £eld campaign. The duration of trial 12 is relatively short, but it may still be of interest due to the special vertical jet release. Deployment of the fast Uvic® concentration sensors and the extent of the temperature measurements and aerosol samples near the source varied. Lidar measurements were included only in trials 23 and 25.

3 Data distribution

The data users of the main Fladis project answered a questionnaire on data needs and preferable distribution methods. The conclusion was that MS-DOS £les were acceptable to everyone, except Electricité de France who later solved their work station compability problem with emulation software. Different degrees of detail were needed; some researchers asked for complete time series whereas others wanted analysed data like the 'average surface concentration at the plume centre line'. Most people preferred *ascii* £les, and it was pointed out that background information, e.g. accurate sensor positions, should be accessible.

data base

The time series are the most voluminous part of the data base, and in spite of the wish of the data users these were compressed to a binary format. All other information are written in *ascii* £les, which may be read by any £le editor. The documentation is divided into general notes and speci£c information for individual trials. The amount of speci£c information varied, but the following three £les were repeated for every trial:

- a description of the release conditions (about 200 words),
- a description of the source (about 20 words), and
- a list of all time series, including sensor position, sample frequency, measured property, physical unit, and a short comment like 'a slight noise from ...' or simply 'ok'.

Block statistics of all time series (mean, standard deviation, maximum, and minimum) are presented as comma-separated *ascii* £les. These may be imported in commercial spreadsheet programs for simple data analyses. The general information include notes on topics

like: surface roughness, instrument response times, a catalog on distributed data, sample programs for reading binary times series (Fortran, Pascal, and C^{++}), and addresses of the experimentalists. Tables which include information from several trials are considered to be general information. Graphics £les with the drawings used in our reports and digitized photographs are included in a separate directory. The data base is further explained in Nielsen et al. (1994).

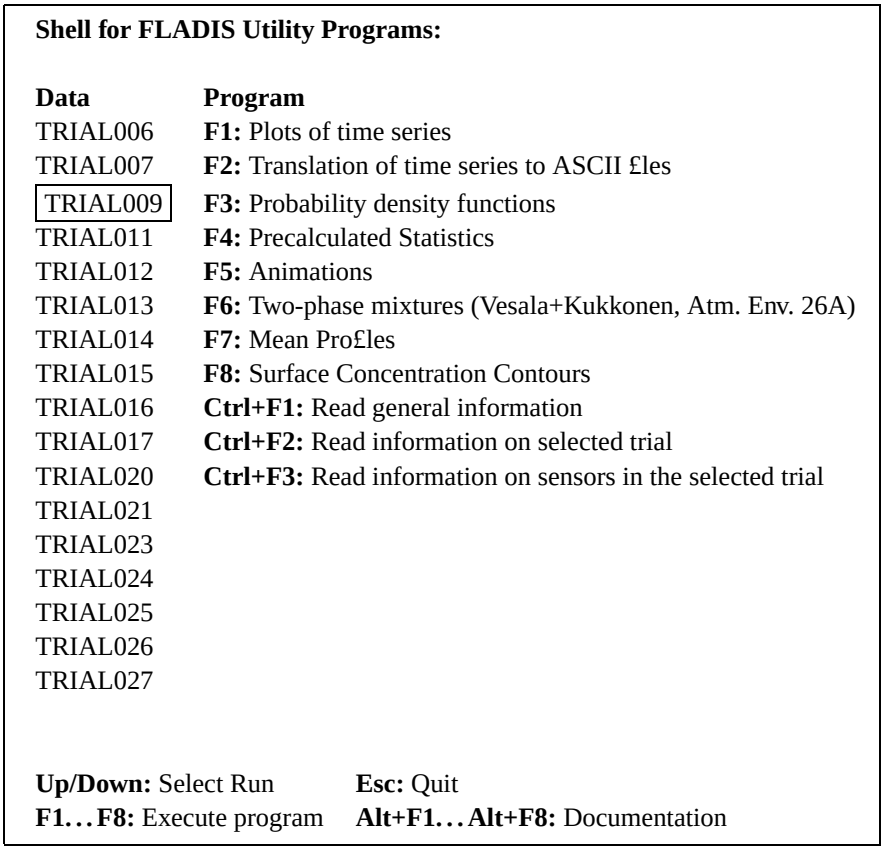

Figure 4. Display of the shell for the distributed utility programs. The up and down arrows are used to select an experiment and the utility programs are executed by pressing one of the hot keys.

utility programs

A set of utility programs are attached to the data base. The programming delayed the data distribution for some months, but it was felt that the analysts would regain the invested time and get a better overview with these tools. A positive side effect was that all time series were inspected and sometimes corrected during this process. Figure 4 shows the main display of a program shell with lists of the available experiments and utility programs. The utility programs are activated by the PC softkeys **F1** to **F8**, which are also used as labels for the following descriptions:

F1 Groups of time series, e.g. signals from a row of concentration sensors, may be plotted on the screen or exported to *hpgl* or *postscript* graphics £les. More than 700 of these plots have been prede£ned and each of them is accompanied by written comments. This system is intended to substitute a lengthy data report.

F2 The researchers who cannot use binary data, may select all or just a few time series and export them into *ascii* £les.

F3 Probability density functions are applicable for the fast concentration and wind velocity measurements. The user is asked to specify the averaging period (with the pedagogic intention to illustrate how sensitive the analysis is to this input).

F4 The precalculated statistics may be viewed from the utility shell.

F5 The computer animations show the variable concentration £eld and sequences of Lidar measurements. The concepts of wind trajectories and moving frame pro£le analysis are demonstrated.

F6 A prediction of the composition of a two-phase mixture of lique£ed ammonia and moist air is adopted from the homogeneous equilibrium limit of the binary aerosol model model by Vesala & Kukkonen (1992).

F7 Plots of average pro£les are organized for different sensor groups. The user may specify the average period, and the mean values are displayed and exported to an *ascii* £le.

F8 Plots of average surface concentration contours are calculated by a Gaussian interpolation model.

Background informations **Ctrl+F1…Ctrl+F3** and documentation on the utility programs **Alt+F1…Alt+F8** may be read from the program shell.

distribution method

The £rst package of data was distributed in a compressed format on six $3\frac{1}{2}''$ disks to a total of 22 organizations. This method was ineff£cient for the large volume of the later data packages which instead were prepared for **ftp** distribution on the internet (for free). At the conclusion of the project the full data set is also available on CD-ROM and MO disks (with a distribution charge). The volume of the installed system is 122 MB distributed on 20740 £les.

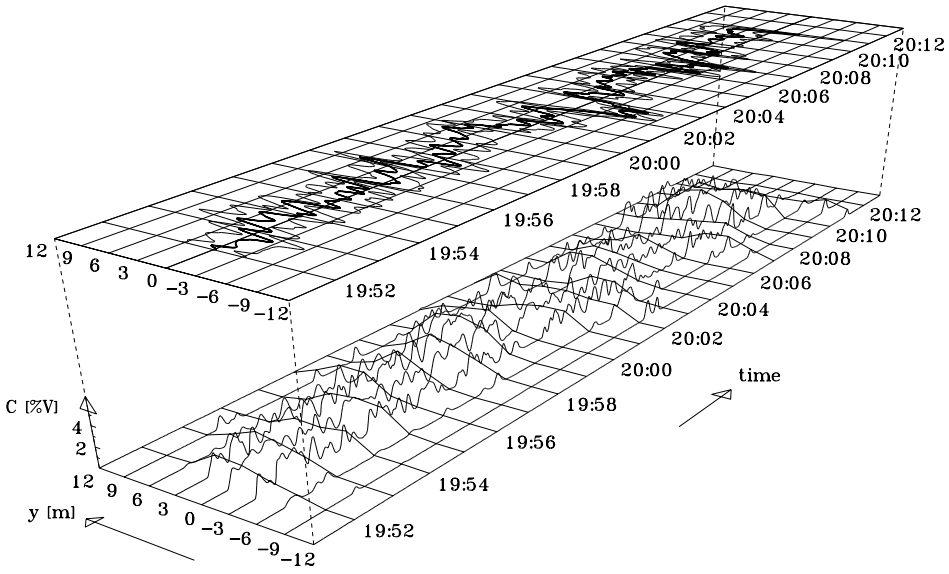

Figure 5. Concentration time series from trial 16. The map above the series shows the instantaneous plume centre line and lateral spreading.

4 Data analysis

Most of the results in this chapter are taken from a paper (Nielsen et al. 1997) which has been submitted to Journal of Hazarduous Materials. The results are described here in a shorter form.

4.1 Plume dimensions

Figure 5 shows a set of concentration time series from the lowest level of the £rst sensor array. The variable plume position and width are shown in the map above the time series. The release lasted 20 minutes, and the plume was sweeping from side to side with about two excursions per minute.

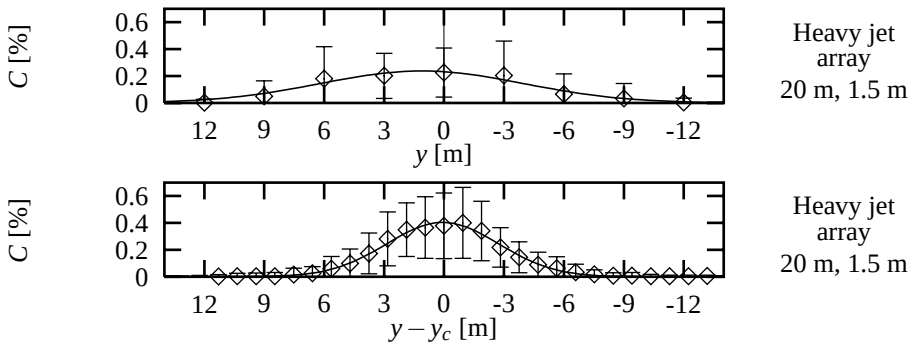

Figure 6. Average concentration pro£les in trial 16 plotted in a £xed frame of reference and moving frame following the position of the instantaneous plume centre line y_c.

Figure 6 shows concentration statistics by similar instruments at the 1.5-m level of the £rst sensor array. In the top frame, the mean and standard deviation of each signal is plotted as a function of the cross-wind distance y. The Gaussian pro£le £tted to the average values seems to describe the concentration distribution quite well. The plot in the lower frame is a different presentation of the same measurements. Here, the observations are sorted into bins depending on the distance to the instantaneous plume centre line $y - y_c$, i.e. in a frame of reference moving with the plume. The moving frame pro£le is also of a Gaussian shape, but the centre-line concentration is higher and the plume is narrower. The ratio between the local standard deviation and average value is comparatively small, i.e. the concentration ¤uctuations are more predictable when the plume position is known. The Gaussian pro£les are convenient for data-reduction purposes, and they have been calculated for all cases where the average plume centre line was inside the sensor array, see table 3 in appendix A. The Gaussian £ts were made with an iteration which compares the moments of a stepwise linear interpolation between the observations to the moments of a clipped Gaussian pro£le (Nielsen 1996b). Most heavy-gas dispersion models assumes crosswind concentration pro£les with a ‘top hat’ shape with or without smooth edges. The reasons for the near-Gaussian shape of the pro£les in these experiments are probably the initial strong jet momentum and further downstream the moderate gravity effect.

discussion

Presumably, the plume dimensions in most heavy-gas dispersion models are consistent with average concentrations without plume meandering. The moving frame analysis should therefore be of most interest in the heavy-gas phase. However, a longer average time e.g. 10 min, is usual in dispersion models for passive diffusion, and many heavy-gas models are designed with a smooth transition to this limit. The best data analysis for a model comparison should depend on the individual model assumptions. The data reduction for the heavy gas model evaluation of Hanna et al. (Hanna & Chang 1991) applied £xed frame analysis, but most of the collected experiments had relatively short release durations. An experiment like Fladis trial 9 would probably have been rejected by these authors, since the changing wind direction during this trial resulted in a very broad £xed frame pro£le. The wind direction in wind tunnels is much more steady than in the atmosphere, and the moving frame analysis is expected to compare better with laboratory measurements.

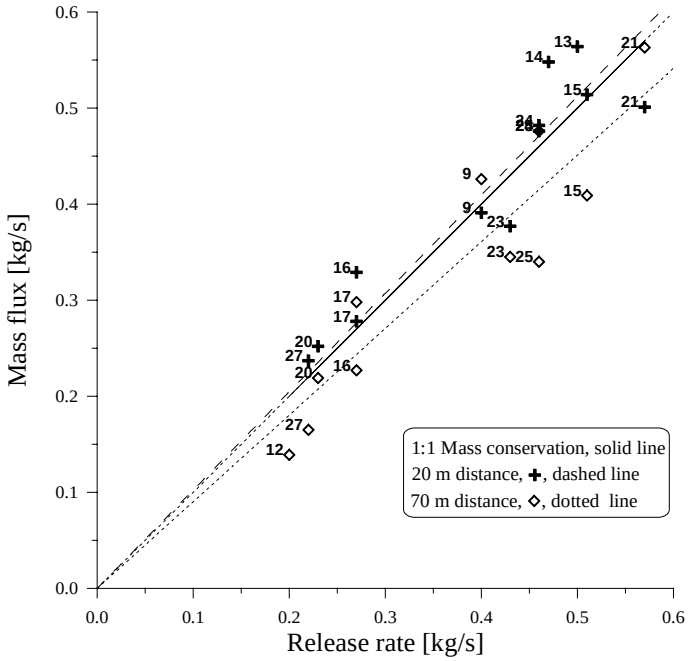

Figure 7. Mass balance between £eld and source measurements.

4.2 Mass balance

Figure 7 shows a comparison of release rates and mass ¤ux estimates from the £eld measurements. The mass ¤uxes are derived from a concentration distribution which is assumed to be Gaussian in the horizontal direction and exponential in the vertical direction. The advection velocity is the measured logarithmic wind pro£le plus a correction for jet momentum (Nielsen et al. 1997). The average mass balance is examined by regression lines through data from many trials. The correlation is found to be 89% for the sensor array at 20-m distance and 84% for the array at 70 m. This is better than the mass balance of the Desert Tortoise experiments (Goldwire et al. 1985), but it should be mentioned that our procedure makes certain extrapolations and we included only cases where both horizontal and vertical plume dimensions are available from table 3. One might contemplate whether the systematical low mass ¤uxes are due to deposition to the grass[3], but the scatter in the data is too high to draw such a conclusion. Peaks in the concentration measurements are expected to be positively correlated with excess velocity in the jet region. This suggests a forward turbulent gas ¤ux which probably improves the mass balance at the 20-m distance.

4.3 Interpolated surface concentrations

Figure 8 illustrates an interpolation method for average surface concentration £elds. The procedure is to

1. calculate average concentrations for a given period,
2. extrapolate the average values to ground level,

[3]The grass withered in the plume footprint and a few months later it seemed more vigorous, probably due to fertilazation.

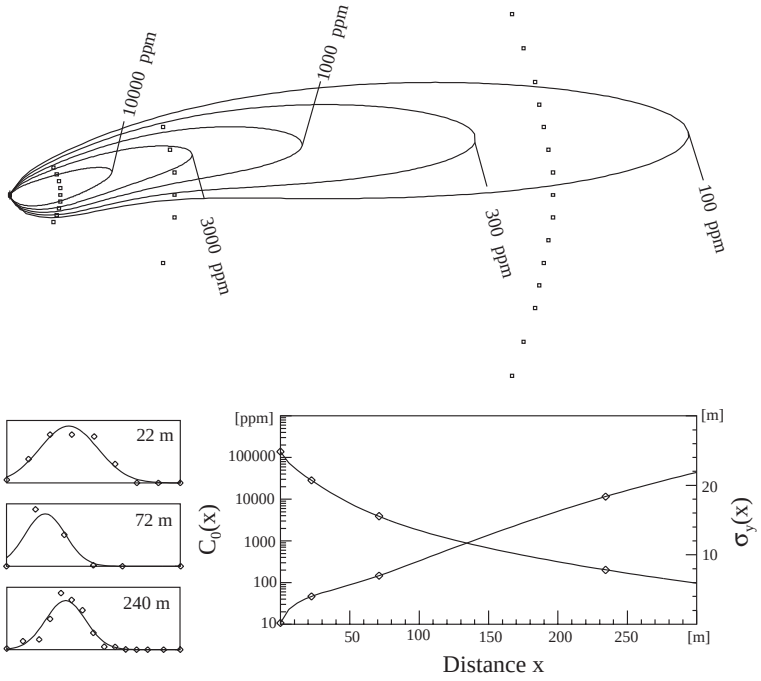

Figure 8. Contour plot of average surface concentrations in a 1-min period of trial 16.

3. £t a Gaussian pro£le to each measurering chain, i.e. determine the plume parameters: center-line position y_c, maximum concentration $c_{\max}$, and plume spreading σ_y,
4. £nd longitudinal spline functions for these plume parameters, and
5. interpolate the concentration contours.

This analysis was inspired and sponsored by Norsk Hydro. It was implemented as the interactive MS-DOS program *contour.exe* and documented in Nielsen (1996b). The purpose was to examine to what extent the average surface concentrations depend on the averaging period. With a short average time the plume footprint will often curve as in £gure 8. For longer averaging times, the meandering plume position will result in a more symmetric but wider and shorter footprint. The analysis showed that these changes were O(10)% when the averaging period was extended from 0.5 min to 10 min, but the footprint area was relatively insensitive to the choice of averaging time.

4.4 Concentration ¤uctuations

Figure 9 shows a concentration time series measured by a fast responding Uvic® sensor. Relatively long quiescent periods are observed when the plume moves away from the sensor. Concentration ¤uctuations inside the plume are sometimes rapid as shown by the close-up frame in the lower part of the £gure. Spectral analysis of Uvic® time series followed the -5/3 power law, which characterize turbulence with an inertial subrange and showed no sign of instrumental smoothing (Nielsen et al. 1997).

probability functions

The plots on the left-hand side of £gure 10 show cumulated probabilities $P\{C \leq c\}$ where each of the concentration signals is regarded as a stochastic variable C. It is noted that the probability of zero concentration increases with the height of observation. The curve added to each plot is a simple model which assumes a £nite probability of zero concentration and a gamma distribution for the non-zero concentrations (Nielsen et al. 1997). The plots on the right hand-side of the £gure are conditional probabilities depending on the distance between the mast and the instantaneous plume centre-line position $|y - y_c|$.

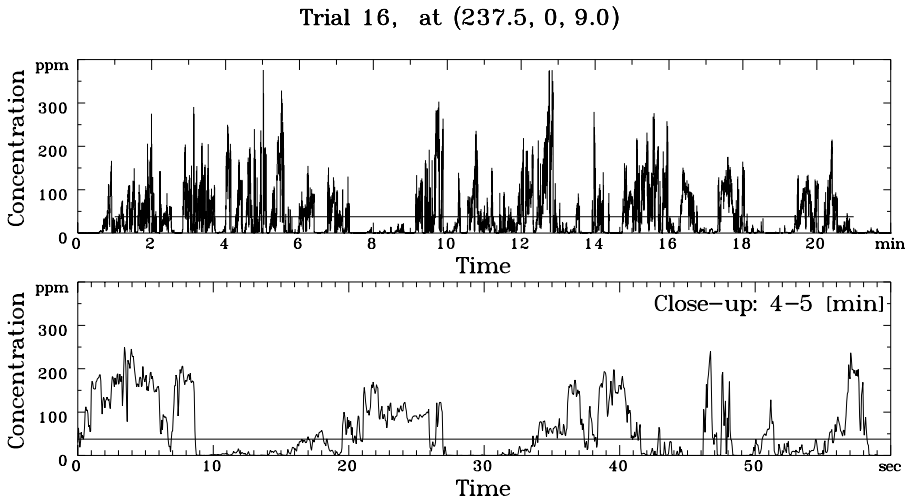

Figure 9. Concentration measured by a fast sensor. The time series at the bottom is a close-up of the above one.

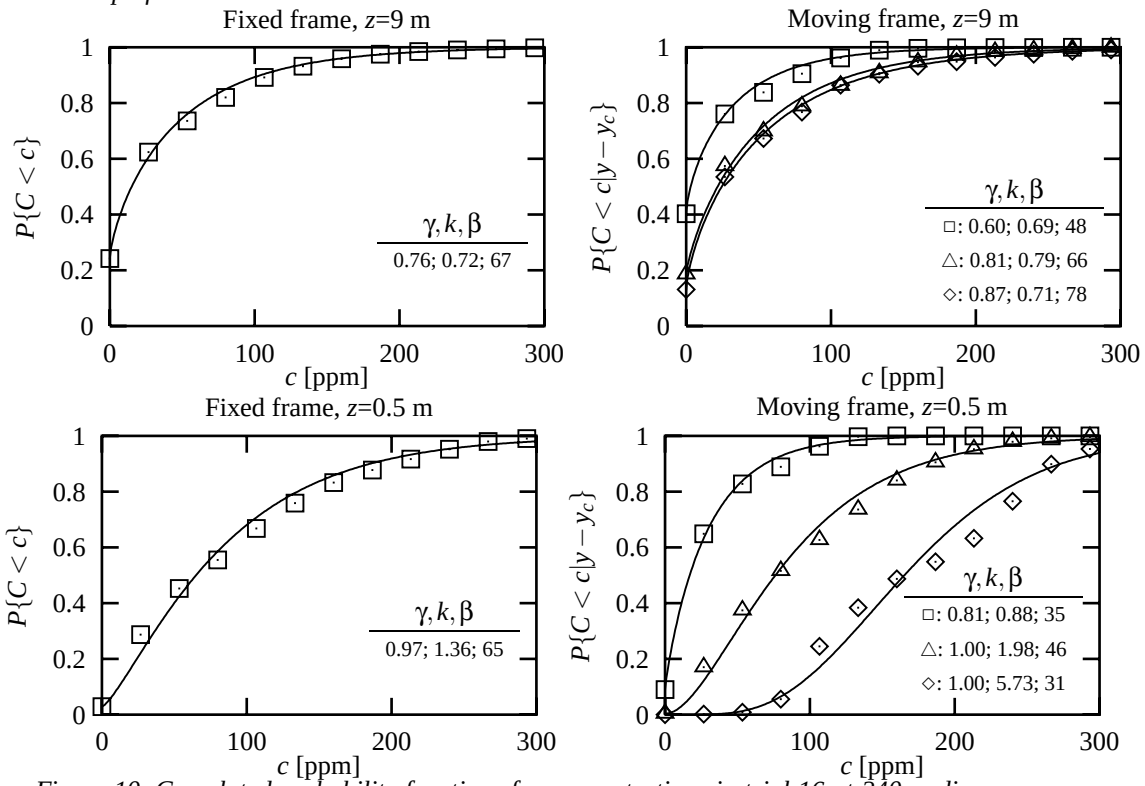

Figure 10. Cumulated probability functions for concentrations in trial 16 at 240-m distance. The plots to the right hand-side show condition probabilities depending on the distance from the mast to the instantaneous plume centre line. These distributions are marked ◇ for $|y-y_c| \le \sigma_y$, + for $\sigma_y < |y-y_c| \le 2\sigma_y$, and □ for $2\sigma_y < |y-y_c| \le 3\sigma_y$.

The probability of high concentrations increases when the plume centre line is close to the mast. This dependence on plume position decreases with height.

spatial correlation

In trial 20 the fast concentration sensors were arranged for a study of the spatial structure of concentration ¤uctuations. The instruments were aligned in the cross-wind direction and separated by irregular spacings. Figure 11 shows the normalized spatial correlation function of the two signals $c(y)$ and $c(y+\delta y)$ for multiple combinations of sensors. The curve added to the £gure is a best £t of the type $R = \exp\{-(\delta y/b)^a\}$ obtained by linear regression of transformed variables. The value of b probably relates to the plume

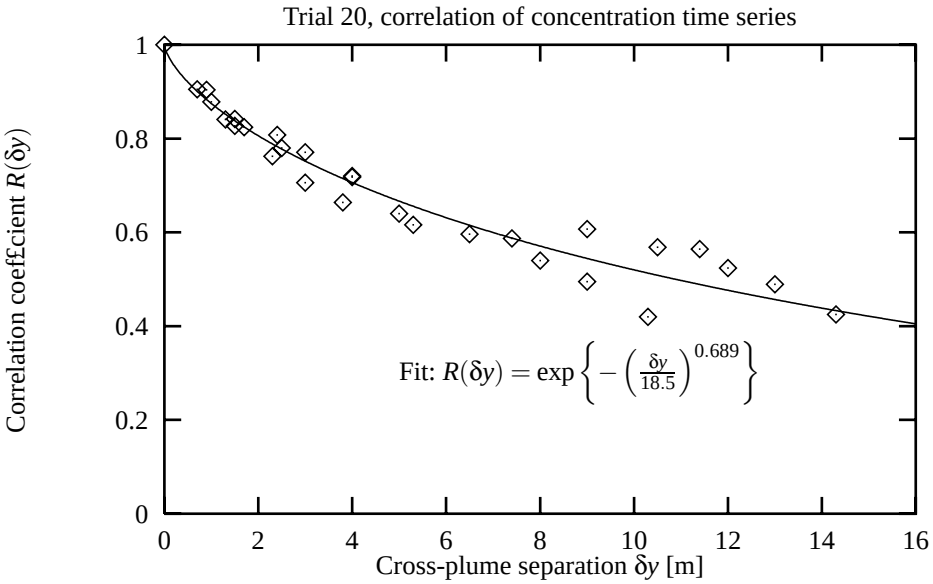

Figure 11. Spatial correlation between concentration measurements by fast sensors distributed perpendicular to the wind direction 230 m from the source at 2-m height.

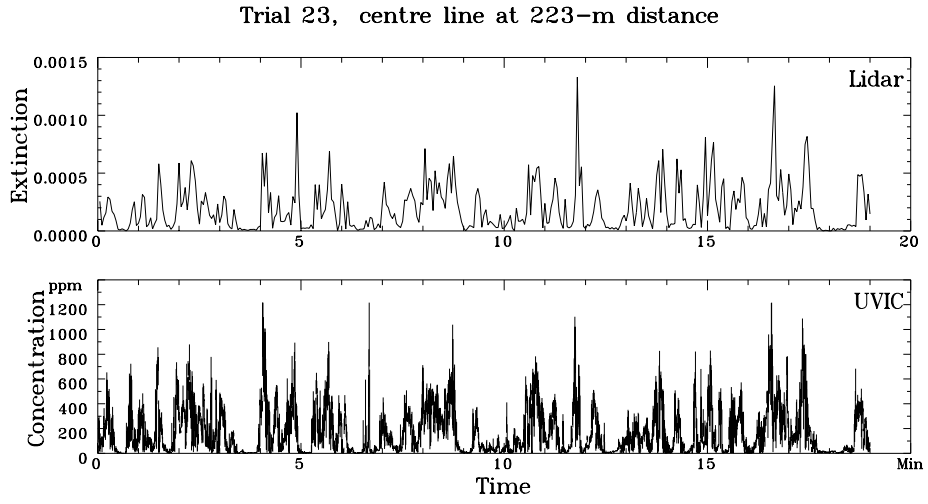

Figure 12. Comparison of Lidar and Uvic measurements.

dimension whereas the exponent *a* may be of more fundamental interest.

Lidar–Uvic comparison

The Lidar measurements in trials 23 and 25 were made with the laser beam just in front of a line of fast Uvic® sensors. Figure 12 compares a Lidar time series constructed from a virtual Lidar measurement point just in front of one of the concentration sensors. Not all peaks of the two time series coincide. This is mainly because the Uvic® time series contains 60 times as many data points as the Lidar time series.

Lidar pro£les

Figure 13 shows ten instantaneous Lidar pro£les measured with intervals of 3 seconds. This time increment corresponds to a plume advection of approximately 10 m. The shapes of the pro£les are far from Gaussian and the plume is sometimes better described as several parallel traces. A trace of gas is often located at the same distance for a long time, e.g. at a distance of −30 m in pro£le number 3 to 8. Sometimes a trace suddenly appears at a new location, e.g. at a distance +40 m in pro£le number 5. Topological explanations for this behaviour are either that the plume lifts off at one distance and lands at another,

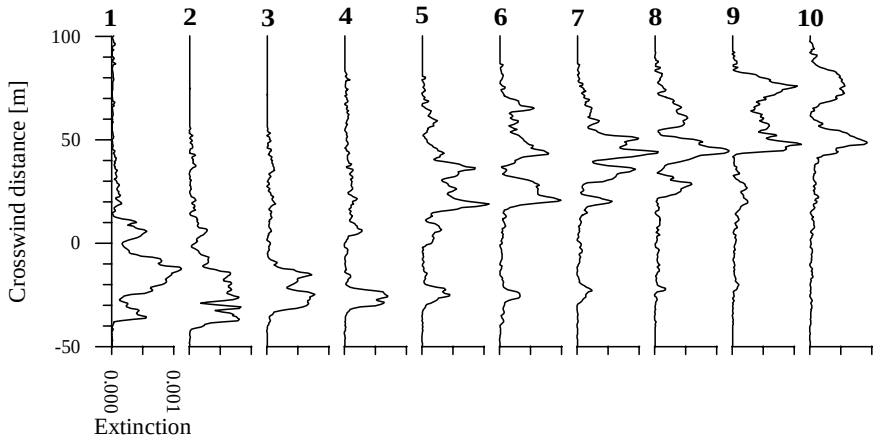

Figure 13. Instantaneous crosswind Lidar pro£les measured with intervals of 3 seconds in trial 25.

or that the plume is broken in two pieces by a sudden change of the wind. The latter explanation seems most likely.

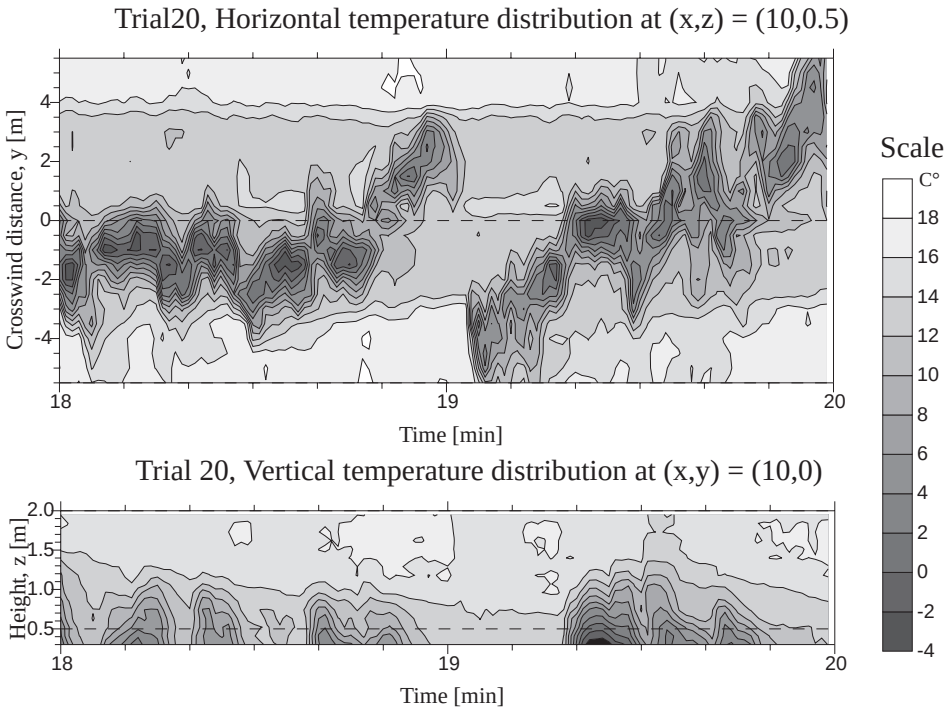

Figure 14. Temperature 10 m from the source as a function of 1) time and cross-wind distance, and 2) time and height above terrain. The contour levels are plotted for increments of 2°C.

4.5 Temperature

The top frame of £gure 14 shows temperature as a function of time and horizontal distance. The measurements were made by 23 thermocouples mounted with 0.5 m separation on a string which was stretched across the cold jet at a height of 0.5 m. The distance was 10 m from the source, and this was just downwind of the point of jet touch-down. The

jet was O(3) m wide and moving vividly from side to side. Steady temperatures $\approx 3^0$C lower than the ambient were observed in a wider space around the jet. However, this is probably a measurering error caused by evaporation of deposit from previous jet exposure. The frame below is a similar plot of measurements by 16 thermocouples mounted with a separation of 0.11 m on a minimast at the ideal centre line. The exposure of the minimast is in accordance with the horizontal position of the plume shown by the upper frame.

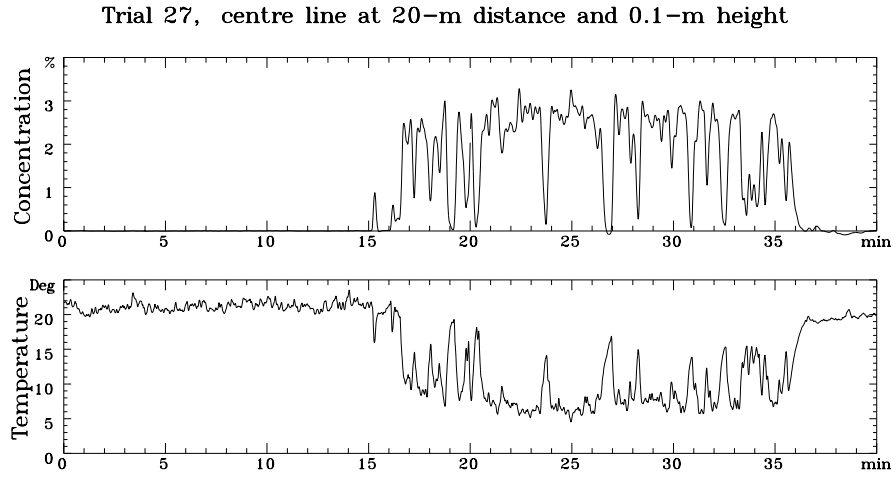

Figure 15. Concentration and temperature from adjacent instruments.

temperature–concentration relationship

Figure 15 is a comparison of concentration and temperature measured by adjacent instruments. The correlation between the two signals is fair, but also at this distance the thermocouple thermometer has a tendency to measure too cold temperatures during short periods with low gas concentration.

adiabatic mixing?

The main cause of the plume temperature de£cit is the enthalpy de£cit of the source. In case of perfect adiabatic mixing the speci£c enthalpy de£cit ΔH and concentration c in the £eld should relate to the initial enthalpy de£cit at the source ΔH_0 by $\Delta H = c \cdot \Delta H_0$. This relation is marked by the solid line in £gure 16. For the pair of sensors at the low level, the observed enthalpy to concentration correlation, determined by the linear regression line, is signi£cantly different from the case of adiabatic mixing. The enthalpy due to condensed aerosols is taken into account, see Nielsen et al. (1997). The result is an indication of heat input from the ground to the cold gas cloud, and it corresponds to a 22% reduction in the density difference relative to the ambient air $\Delta\rho/\rho$.

heat ¤ux

An attempt was made to measure the heat ¤ux from the ground to the gas cloud with a calorimeter (Nielsen et al. 1994). These measurements were inconclusive because a deposit of liquid aerosols made the device cool faster than the heat ¤ux to the cloud. The unknown temperature and mass of the deposit makes a correction impossible. The surface temperature measured by a remote sensing thermometer was found to be substantial lower after gas release than before. However, this is no proof of heat transfer, since the temperature depression might as well be caused by evaporation of the wet surface.

4.6 Aerosol composition

In order to measure the composition of the liquid aerosols, we took samples of the deposit in the release area. The aerosol collectors in trial 15 to 17 were placed along the ideal plume centre line at heights following the path of the jet from 4 to 12-m distance. Figure 17 shows the composition of the sampled material as a function of distance from

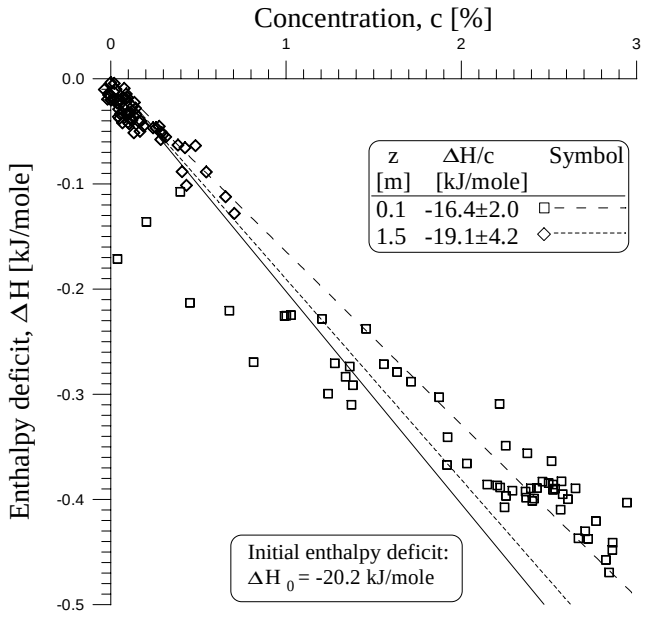

Figure 16. Correlation of 20-sec average enthalpy de£cit and concentration.

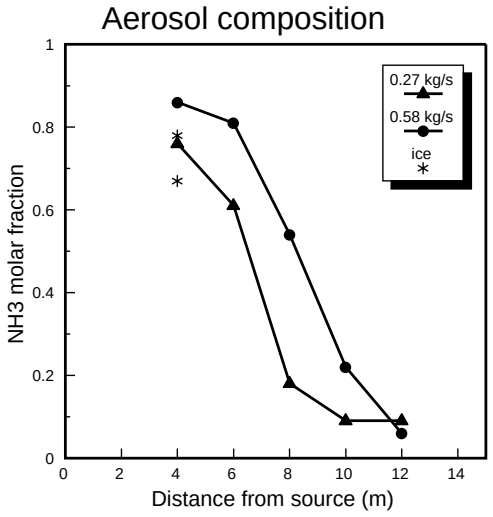

Figure 17. Measured composition of liquid samples in trial 15 ∘ and trial 16 Δ as a function of the distance from the source. The two ice samples ∗ are taken from trial 16 and 17, which both had release rates of ṁ=0.27 kg/s.

the source. The aerosol content is seen to change within a few metres from almost pure ammonia to almost pure water. The jet swept from side to side, i.e. not hitting the collectors all the time, and it took O(1) minute to collect all samples after the release. It is possible that ammonia was lost or water condensed from the atmosphere during periods when the collector was exposed to the ambient air. The ammonia content in samples of ice deposit directly on a rig was, however, comparable to that of the sample in a nearby aluminum envelope. This indicates that ammonia evaporation from the envelopes was not serious.

4.7 External analysis

Researchers of the main Fladis project were able to analyse some of our measurements in spite of the delayed data transfer. This is a short description of their work:

Shef£eld University used fast concentration time series to 1) check the empirical skewness–kurtosis relationship $K = aS^2 + b$ also found in other experiments, and 2) £nd probability density functions for concentration ¤uctuations (Duijm 1994, ch. 8).

Hamburg University made a wind-tunnel simulation of trial 16. According to £gure 3.4 of Duijm (1994, ch. 3), the average concentrations were higher in the wind tunnel, but the applied £eld data were £xed frame statistics, which are affected by more plume meandering than in the laboratory. Moving frame maximum concentrations from table 3 are in better accordance with the HU wind-tunnel data.

Electricité de France and Gaz de France compared the MERCURE model to trial 16, see Gabillard & Carrissimo (1994) and Duijm (1994, ch. 14–15). Similar to the HU wind-tunnel simulation the predicted plume was too narrow with too high maximum concentrations. Again, this is probably due to plume meandering.

NSCR 'Demokritos' compared the near-source temperature–concentration relationship near the source to predictions by the ADREA-HF model (Duijm 1994, ch. 16). It was concluded that the model had dif£culties with the degree of condensation in the binary water–ammonia aerosols.

Joint Research Centre, Ispra validated the 1D shallow layer model (Würtz 1993) against trial 16 data.

5 Models

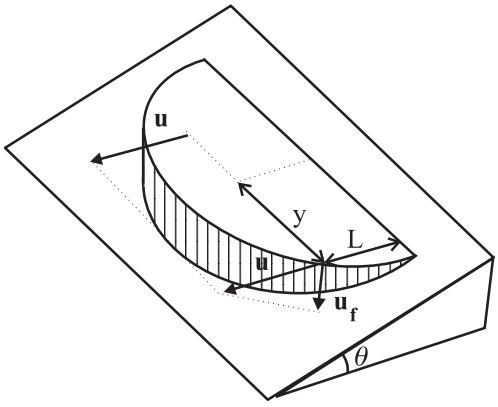

Figure 18. Box model for instantaneous releases on a uniform slope as proposed by Webber et al. (1993)

5.1 Box model for sloping terrain

One of the participants in the main Fladis project used a shallow water model to study the motion of a heavy gas cloud on a uniform slope (Webber et al. 1993). For releases without ambient wind, surface friction or entrainment, the cloud approached a steady wedge shape as shown in £gure 18. This observation inspired the authors to formulate

a box model with a horizontal top surface, and a rear boundary which intersected the terrain. The local front velocity was modelled by the usual front velocity $u_f = Fr_f\sqrt{g'h}$, where h is the local height. In order to maintain a constant shape all velocities in the cloud must be equal. This gives a kinematic condition of the front which leads to the speci£c 'dutch cheese' shape shown in £gure 18.

The model by Webber et al. (1993) was originally developed for a uniform slope, but Nielsen (1996a) generalizes the analytical solution to a V-shaped valley, resulting in the cloud shape sketched in £gure 19. A numerical solution was also found for a valley with a parabolic cross-section.

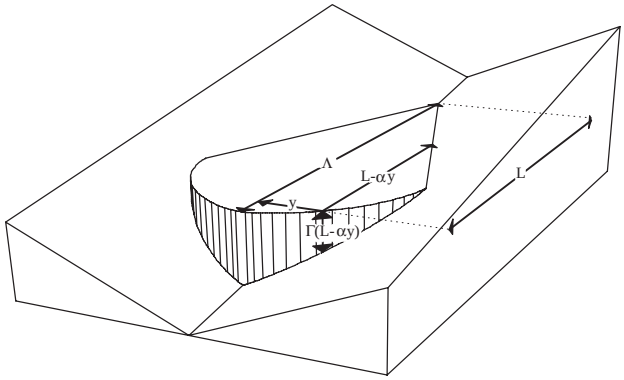

Figure 19. Modi£ed box model in a V-shaped valley.

5.2 The numerical shallow layer model SLAM

In the course of the project a shallow layer model was developed. The model is called SLAM (Shallow LAyer Model), Ott & Nielsen (1996). Shallow layer models are intermediate in complexity between box models and full 3D models. The motivation for making shallow layer models is that they can deal with complex terrain at a modest computational cost compared to 3D codes. They also model the gravity induced ¤ow dynamically. The main disadvantage is that the air-cloud interactions still have to be added 'by hand', where 3D models inherit the correct dynamics from the fundamental equations.

SLAM has some distinct features compared to other shallow layer models, e.g. Würtz (1993):

- The turbulent kinetic energy budget is explicitly accounted for.
- The entrainment rate is estimated on the basis of the local turbulent kinetic energy.
- Non-hydrostatic pressure.
- A Lagrangian grid is used in the numerical solutions.
- Numerical methods ensure that conservation laws are not jeopardized even for coarse grids.

Several prototypes were made, most of them solving 1D problems, and it was recognized that the simple inviscid shallow water equations are dif£cult to solve. It was observed that simple solvers often yield unstable solutions.

Since robustness is an important feature some effort was spent in £nding the cause of these instabilities. It appears that the shallow-water equations do not always have solutions because of the development of fronts or breaking waves. This was demonstrated

by analytical results. Still powerful numerical schemes can yield breaking wavesolutions, such as the ¤ux corrected transport method. The solution to this apparent paradox is subtle. If a friction term with an arbitrarily small diffusivity is added, breaking wave solutions exist. Furthermore, the solutions converge as the diffusivity goes to zero. In other words, an in£nitesimal friction term ensures the existence of solutions. The secret of the ¤ux corrected transport method is to add a small amount of numerical diffusion. However, it matters whether the friction is internal or external, so numerical diffusion has to be carefully controlled. At the same time the implicit introduction of physics into the model via numerical procedures does not seem healthy. It was decided therefore not to use such methods.

It was pointed out that dicontinuities of the hydrostatic pressure at elevated cloud edges induce in£nite accelerations, when using the hydrostatic approximation. The hydrostatic approximation therefore had to be improved.

A closed set of layer-integrated equations, describing budgets for mass, contaminant, momentum and turbulent kinetic energy, was derived starting from the Navier-Stokes equations. This involves a series of manipulations accompanied by plausible arguments.

Like any numerical model the SLAM model consists of a £nite set of equations involving a £nal set of variables. In light of the delicate role played by numerical diffusion, a direct discretization of the continuous equations was not used. Instead it was shown that the shallow-layer equations (*including* friction and entrainment) can be derived from a least action principle. This means that the equations minimize a certain action integral, and the discrete equations were derived from a discrete analog to the action integral. A discrete system of equations constructed in this way will describe a mechanical system, ensuring that conservation laws are not jeopardized. The procedure automatically yields equations in Lagrangian coordinates. Furthermore, it is relatively simple to improve the hydrostatic approximation in this framework. A triangular grid (sectioning the cloud into triangular prisms) was used since this seems to be the simplest possibility.

Thorney Island trial 8 was used as a reference case. This is an instantaneous isothermal release of a Freon/Nitrogen mixture. The entrainment constants were tuned by means of concentration data from sensors located at several heights in order to reproduce the doughnut shape of the cloud. The results are in reasonable agreement with observations, even when a small number of cells (e.g. 16) is used.

Further data comparison is needed to validate the model.

6 Further aspects

Supporting studies were undertaken by CERC. In the £rst study (Edmunds & Britter 1994) it was found that the building adjacent to the test site may have had an in¤uence on the £eld results, and this possibility should be considered when interpreting the £eld data. In the second study (a Britter 1994, Britter 1995)n extensive review and analysis of the modelling of ¤ashing releases was undertaken. In particular it was deduced that there is considerable misunderstanding in the literature and that direct application of the fundamental equations of ¤uid mechanics and thermodynamics leads to unambiguous conclusions (at least for somewhat idealized scenarios). In a third study Britter (1996a) compares different entrainment correlations used in heavy-gas dispersion models. This detail is a vital part of ‘box’-type models but apparently no consensus has been reached. The entrainment function must be chosen in accordance with the parametrization of the vertical concentration distribution. Finally, Britter (1996b) gives an overview of the connections between the main Fladis project and the Fladis £eld experiements.

7 Conclusions

measurement quality

The release nozzles were designed for measurements of initial enthalpy, release rate, and jet momentum. These parameters are often uncertain in heavy-gas £eld experiments. The release rates agreed within 5% of the total mass of the release amount of ammonia. The average plume mass ¤ux, estimated from £eld measurements at 20 and 70-m distance, was O(85)% of the release rate. Unfortunately, the masts were too short for an accurate determination of the plume height at 238-m distance. New fast concentration sensors were used, and the spatial structure of the plume was monitored by a remote sensing Lidar. A large number of meteorological instruments were applied, and the atmospheric stability and friction velocity were found by eddy correlation of turbulence measurements, i.e. more accurately than by gradient-based methods.

new analyses

Gaussian pro£les were £tted to horizontal average pro£les in a £xed frame of reference and relative to the instantaneous plume centre line. Plume meandering is not always included in numerical or physical models. The moving frame statistics should therefore be more applicable for model evaluation and probably also for risk analysis. A method for interpolating plume footprints was developed. This should be applicable for dispersion experiments with similar sensor con£gurations in chains across the plume. An molar weight appropriate for producing similardensity effects with isothermal gas release is proposed.

new results

We have measured the change of aerosol composition in the two-phase jet with the distance from the source. An enthalpy budget suggests that the mixing was not adiabatic (due to heat ¤ux from the ground), and this could reduce the density difference from the ambient air with O(20)%. The length of the 500 ppm plume footprint changed with O(10)% when the average period was increased from 0.5 to 10 min. This means that the concept of a ‘lower ¤amability distance’ popular in risk assessment has a systematic dependance on the average period. A spatial correlation of in-plume concentration ¤uctuations was deduced. The plume was not observed to lift off the ground.

data dissemination

The documentation and data dissemination were considered to be an important aspect of the work. The instruments, data acquisition, and signal processing are described in a report and £les distributed together with the data. Care has been taken also to document changes particular for the individual trial. A set of utility programs for data browsing and analysis is included.

external analysis

The data are structured in a way which allows analysis with different degrees of details:

- The release conditions in table 2 and the average concentration pro£les in table 3 of appendix A may be used for preliminary model evaluation.
- The precalculated block statistics distributed with the data are easy to import in commercial spreadsheet programs.
- The access to time series enables sophisticated analyses.

It may be of interest for model evaluators to know that the Rediphem data base (Nielsen & Ott 1995) contains time series from many heavy-gas £eld and wind-tunnel experiments including Fladis.

model development

A new shallow layer model SLAM was developed. The numerical solution of SLAM was obtained by a Lagrangian grid following the heavy gas cloud. No ‘hydrostatic pressure assumption’ was made, and the entrainment rate was based on local turbulent kinetic energy budgets. The ‘box’ type model of Webber et al. (1993) for heavy gas dispersion on a uniform terrain was generalized for dispersion in a V-shaped valley.

publications

Appendix B contains a list of material produced during this project.

Acknowledgement

Participants in the project were:

Risø: M. Courtney, M. Frederiksen, O. Frost, A. Hansen, J. Holm, H. E. Jørgensen, S. Lund, B. Mogensen, J. Nielsen, M. Nielsen, S. Ott, and V. Thøfner

Hydro-Care: B.J. Andersen, R. Bengtsson, S. Björk, B. Kyngsman, and B. A. Tegner

FOA: M. Nordstrand, K. Nyrén, and S. Winter

CBDE: S.C. Cheah, W.S. Evans, T.J. Higgs, C. Jones, and D. Ride

CERC: R.E. Britter and H.A. Edmunds

The main sponsors were CEC DG XII ENVIRONMENT Programme Contract No. EV5V–CT92–0069 and NUTEK Contract No. D52266–92–11821 (FOA & Hydro-Care). Additional funding was provided by the Swedish Rescue Board (FOA) and Norsk Hydro Contract No. PR5–23149.01 (Risø).

References

Britter, R. E. (1994). The modelling of a pseudo-source for complex releases, *FM89/2*, Cambridge Environmental Research Consultants.

Britter, R. E. (1995). A further note on modelling ¤ashing releases, *FM89/3*, Cambridge Environmental Research Consultants.

Britter, R. E. (1996a). Comparison of entrainment correlations in dense gas dispersion models, , Cambridge Environmental Research Consultants. in preparation.

Britter, R. E. (1996b). Fladis and Fladis £eld project connections, , Cambridge Environmental Research Consultants. in preparation.

Britter, R. E. & McQuaid, J. (1988). Workbook on the dispersion of dense gases, *Contract research report 17/1988*, Health and Safety Executive.

Builtjes, P. J. H. (1992). Research on continuous and instantaneous heavy gas clouds, *92-135*, TNO Environmental and Energy Research.

Duijm, N. J. (1994). Research on the dispersion of two-phase ¤ashing releases – Fladis. Fladis £nal report., *R94-451*, TNO Environmental and Energy Research.

Edmunds, H. A. & Britter, R. E. (1994). The effect of nearby buildings on a passive release, *FM89/1*, Cambridge Environmental Research Consultants.

Gabillard, M. & Carrissimo, B. (1994). Project Fladis - Pressurized ¤ashing releases - Part III: Ammonia releases: Comparison of 3-D Mercure results against experiments (Trial 016), *M.CERMAP–941.640*, Gaz de France.

Goldwire, H. C., McRae, T. G., Johnson, G. W., Hipple, D. L., Koopman, R. P., McClure, J. W., Morris, L. K. & Cederwall, R. T. (1985). Desert Tortoise series data report – 1983 Pressurized ammonia spills, *UCID-20562*, US Lawrence Livermore National Laboratory.

Hanna, S. R. & Chang, J. C. (1991). Uncertainties in hazardous gas model predictions, *AIChE International Conference and Workshop on Modeling and Mitigating the Consequences of Accidental Releases of Hazardous Materials – New Orleans, May 20–24 1991*, 345–368.

Heinrich, M. & Scherwinski, R. (1990). Propane releases under realistic conditions – Determination of gas concentrations considering obstacles, *Report 123UI00780*, TÜV Norddeutchland e. V.

Jørgensen, H. E. & Mikkelsen, T. (1993). Lidar measurements of plume statistics, *Boundary-Layer Meteorol.*, **62**, 361–378.

König-Langlo, G. & Schatzmann, M. (1991). Wind tunnel modeling of heavy gas dispersion, *Atmos. Environ.*, **25A**, 1189–1198.

Nielsen, M. (1996a). Comments on 'A model of the motion of a heavy gas cloud released on a uniform slope', *J. Hazard. Mater.*, **48**, 251–258.

Nielsen, M. (1996b). Surface concentrations in the FLADIS £eld experiments, *Risø-I-995(EN)*, Risø National Laboratory.

Nielsen, M., Bengtsson, R., Jones, C., Nyrén, K., Ott, S. & Ride, D. (1994). Design of the Fladis £eld experiments with dispersion of liqui£ed ammonia, *Risø-R-755(EN)*, Risø National Laboratory.

Nielsen, M. & Jensen, N. O. (1991). Continuous release £eld experiments with obstacles, *Risø-M-2923*, Risø National Laboratory. Final report on project BA. X2. CEC DG. XII contract No. : EV4T 0012-DK (B).

Nielsen, M., Jensen, N. O. & Ott, S. (1990). Turbulence in a dense gas mixing layer, *Ninth AMS Symposium on Turbulence and Diffusion, American Meteorological Society, Roskilde Denmark, 30 April – 3 May*, 145–148.

Nielsen, M. & Ott, S. (1995). A collection of data from dense gas experiments, *Risø-R-845(EN)*, Risø National Laboratory.

Nielsen, M., Ott, S., Jørgensen, H. E., Bengtsson, R., Nyrén, K., Winter, S., Ride, D. & Jones, C. (1997). Field experiments with dispersion of pressure lique£ed ammonia, *J. Hazard. Mater.*, **56**, 59–105.

Nyrén, K. & Winter, S. (1987). Discharge of condensated sulfur dioxide: A £eld test study of the source behaviour with different release geometries, *J. Hazard. Mater.*, **14**, 365–386.

Nyrén, K. & Winter, S. (1990). Pressure measurements on the release system and determination of jet momentum in the project BA propane £eld tests 1989, *report E40044*, Swedish Defense Research Establishment. ISSN 0281-9945.

Ott, S. & Nielsen, M. (1996). Shallow layer modeling of dense gas clouds, *Risø-R-901(EN)*, Risø National Laboratory.

Pfenning, D. B., Millsap, S. B. & Johnson, D. W. (1987). Comparison of turbulent jet model predictions with small-scale pressurized releases of ammonia and propane, *in* J. Woodward (ed.), *Proc. International Conference on Vapor Cloud Modeling, November 2–4, Boston, USA*, AIChE, 81–115.

Resplandy, A. (1969). Étude expérimetale des propriétés de l´ammoniac, *Chim. Ind. Genie Chim.*, **102**(6), 691–702. (In French).

Vesala, T. & Kukkonen, J. (1992). A model for binary droplet evaporation and condensation, and its application for ammonia droplets in humid air, *Atmos. Environ.*, **26A**(9), 1573–1581.

Webber, D. M., Jones, S. J. & Martin, D. (1993). A model of the motion of a heavy gas cloud released on a uniform slope, *J. Hazard. Mater.*, **33**, 101–122.

Würtz, J. (1993). A Transient One-dimensional Shallow Layer Model for Dispersion of Denser-Than-Air Gases in Obstructed Terrain under Non-Isothermal Conditions, *EUR 15343 EN*, Commision of the European Communities Joint Research Centre.

Table 3. Centre-line concentration $c_{\max}$, plume spreading σ_y at distance x_r and height z_r. The primary values are moving frame statistics, whereas values in parenthesis are £xed frame statistics. Also shown are: The vertical centre of mass $\overline{z}$ and the ratio between the individual observation period T_{obs} and the release duration T_{dur}.

	x_r [m]	z_r [m]	$c_{\max}$ [ppm]	σ_y [m]	$\overline{z}$ [m]	$T_{\text{obs}}/T_{\text{dur}}$
Trial 9	20	0.1	19600 (12800)	2.66 (4.08)	0.95	1.03
	70	0.5	2050 (885)	5.70 (15.5)	3.32	1.03
	238	1.5	138 (57)	13.6 (37.6)	?	1.04
Trial 12	16	0.1	10300 (7740)	4.03 (5.04)	1.13	< 1
(vertical)	66	0.5	1180 (1010)	12.6 (16.1)	2.65	1.03
Trial 13	22	0.1	24800 (21200)	3.53 (4.03)	0.91	< 1
	72	0.5	1970 (1700)	7.65 (7.65)	?	< 1
Trial 14	22	0.1	24000 (20700)	3.50 (3.93)	0.92	1.06
	72	0.5	1790 (1660)	8.06 (8.83)	?	1.03
Trial 15	22	0.1	26200 (20700)	2.90 (3.58)	0.85	1.08
	72	0.5	2360 (1710)	7.21 (10.3)	?	1.06
	240	1.5	166 (127)	19.0 (26.9)	?	1.28
Trial 16	22	0.1	21300 (16700)	3.38 (4.27)	0.83	< 1
	72	0.5	1810 (1090)	6.77 (11.7)	2.62	< 1
	240	1.5	179 (127)	16.7 (25.3)	?	1.05
Trial 17	22	0.1	19200 (16900)	3.54 (3.88)	0.83	1.06
	72	0.5	1570 (1380)	7.68 (7.26)	?	< 1
Trial 20	20	0.1	21600 (12900)	3.00 (4.84)	0.78	1.02
	70	0.5	1140 (583)	8.86 (18.6)	3.21	< 1
Trial 21	20	0.1	37600 (30100)	3.05 (3.72)	0.78	1.01
	70	0.5	5910 (3600)	7.86 (12.9)	1.85	1.02
Trial 23	20	0.1	20400 (15100)	2.46 (3.22)	0.91	1.03
	70	0.5	1880 (1250)	6.97 (10.4)	?	1.02
	238	1.5	92 (62)	20.7 (31.9)	?	1.02
Trial 24	20	0.1	31700 (26400)	3.21 (3.65)	0.77	1.08
	70	0.5	2560 (1690)	8.57 (14.0)	2.59	1.08
	238	1.5	113 (74)	24.7 (40.2)	?	1.13
Trial 25	20	0.1	33700 (29000)	3.30 (3.59)	0.76	1.03
	70	0.5	3270 (2040)	7.73 (12.6)	2.00	1.00
	238	1.5	146 (98)	21.3 (32.9)	?	1.03
Trial 26	20	0.1	16100 (12800)	3.98 (4.70)	0.72	1.05
	70	0.5	724 (608)	10.1 (11.4)	?	< 1
Trial 27	20	0.1	25200 (19500)	4.60 (5.54)	0.62	1.07
	70	0.5	1850 (951)	8.60 (16.3)	2.58	1.08
	238	1.5	24 (12)	21.0 (51.7)	?	< 1

A Average plume pro£les

Table 3 contains Gaussian curve £ts to average concentrations measured by horizontal chains of sensors at distance x_r and height z_r. This is done for a £xed frame of reference

and a frame of reference moving with the instantaneous plume centre line y_c

$$c \propto \begin{cases} c_{\max,\pounds x} \exp\left[-\dfrac{y^2}{2\sigma^2_{y,\pounds x}}\right] & \text{for £xed frame pro£les} \\ c_{\max,\mathrm{mov}} \exp\left[-\dfrac{(y-y_c)^2}{2\sigma^2_{y,\mathrm{mov}}}\right] & \text{for moving frame pro£les} \end{cases}$$

The vertical distribution was close to an exponential pro£le $c \propto c_0 \cdot \exp[-z/\overline{z}]$. The vertical centre of mass $\overline{z}$ shown in the table is found, however, by stepwise linear interpolation between the measurements and linear extrapolation to the ground. Cases where this estimate deviated too much from the estimate based on exponential curve £t are excluded from the table. This discriminates all values from the 238-m distance, where the masts were simply too short for accurate estimates of the plume height.

The values of the table may be used as a reduced data set for a quick model evaluation. The question of whether to use £xed or moving frame statistics must depend on the speci£c model concepts. The moving frame pro£les are probably the most accurate ones and it should be remembered that the £xed frame analysis has been done by integration over a variable release duration.

Nielsen (1996b) discuss how to interpolate the concentration £eld between the measurering chains and the source, and prefers to

1. transform concentrations to a logarithmic scale $\ln c$,
2. transform the downwind distance to a coordinate system with equidistant spacing of the measurering chains, and then
3. apply natural cubic spline for the longitudinal variation of centre-line position y_c, centre-line concentration $c_{\max}$, and plume spreading σ_y.

The interpolated values will be more uncertain than the values in the measurering chains.

B List of published material

- An accessible data base with measurements from the best of our experiments, i.e. the ones listed in table 2. This includes background documentation and software for data browsing and analysis.
- A report documenting the experimental design (Nielsen et al. 1994).
- A report on the effects of upstream buildings as estimated by the ADMS passive dispersion model (Edmunds & Britter 1994).
- A report on plume footprint and the in¤uence of averaging time (Nielsen 1996b). This is distributed together with the interactive MS-DOS program *contour.exe*.
- A VHS video with 15 min from the present experiments, plus 7.5 min from the previous propane experiments. This is intended mainly for data users.
- An overview article illustrating most aspects of the experiments (Nielsen et al. 1997).
- A report on the appropriate molar weight for pseudo gas sources in wind-tunnel simulations of pressurized gas releases (Britter 1994).
- A report discussing whether assumptions or isenthalpic of isotropic expansion are necessary when modelling ¤ash boiling jets (Britter 1995).
- A report discussing entrainment correlations (Britter 1996a).

- A report on the connection between the main Fladis project and the present Fladis Field Experiments (Britter 1996b).
- A short article (Nielsen 1996a) which generalizes the heavy gas box model for uniform slopes (Webber et al. 1993) to valleys with a uniform cross-section.
- A report documenting the new shallow layer model SLAM (Ott & Nielsen 1996).
- An internet presentation at

  http://www.risoe.dk/amv/amv_tuf/densegas/densegas.html

C List of project partners

Risø Risø National Laboratory, AMV-125
P.O. Box 49, DK-4000 Roskilde, Denmark
Contact: Morten Nielsen, E-mail: metmn@risoe.dk
Tel: +45.4677.5022, Fax: +45.4675.5619

Hydro-Care Hydro-Care Industrial Safety Academy (now ESQ Management)
P.O. Box 516, S-26124 Landskrona, Sweden
Contact: Roland Bengtsson
Tel: +46.418.76100, Fax: +46.418.17094

FOA Swedish Defense Research Establishment
Cementvägen 20, S-90812 Ume, Sweden
Contact: Stellan Winter, E-mail: winter@ume.foa.se
Tel: +46.9010.6600, Fax: +46.9010.6800

CBDE Chemical & Biological Defense Establishment
P.O. Box 37, Salisbury SP4 0JQ, United Kingdom
Contact: Chris Jones
Tel: +44.1980.613.298, Fax: +44.1980.613.311

CERC Cambridge Environmental Research Consultants Ltd.
Kings Parade 3D, Cambridge CB2 1 SJ, United Kingdom
Contact: Rex Britter, E-mail: rb11@eng.cam.ac.uk
Tel: +44.1223.357.773, Fax: +44.1223.357.492

Bibliographic Data Sheet **Risø–R–898(EN)**

Title and author(s)

Fladis Field Experiments – Final Report

Morten Nielsen and Søren Ott

ISBN	ISSN
87–550–2184–0	0106–2840

Dept. or group	Date
Meteorology and Wind Energy	June 1996

Groups own reg. number(s)	Project/contract No.
TUF–02800–00	CEC D.G. XII EV5V–CT92–0069

Pages	Tables	Illustrations	References
34	3	19	29

Abstract (Max. 2000 char.)

Abstract The objective of the Fladis £eld experiments was to investigate dispersion of lique£ed ammonia with equal attention to the near-source aerosol jet, the intermediate heavy gas dispersion phase, and the downstream transition to passive dispersion. The present report presents the sensor layout and gives an overview of the available experimental data. The average concentration £eld is parametrized by Gaussian distributions. This is done for observations in a £xed frame of reference and relative to the instantaneous plume centre line. The moving frame statistics are expected to compare better with wind tunnel simulations and numerical models which do not include plume meandering. The plume mass ¤ux is estimated from the observed plume pro£les and compared to the release rate. Average surface concentrations are found with a special interpolation method, and this is used to study how the averaging period affects the plume footprint. The instantaneous plume is non-Gaussian, and this is demonstrated by Lidar measurements in the far £eld and thermocouple measurements in the near-source jet. Probability functions and a spatial correlation for the concentration are found. The heat budget of the plume shows signs of heat ¤ux from the ground. The composition of the liquid aerosols was observed to change from almost pure ammonia to almost pure water.
A new two-dimensional ‘shallow layer’ type model SLAM is developed, and an existing ‘box’ type model for heavy-gas dispersion on a uniform terrain is generalized.

Descriptors INIS/EDB

AEROSOLS; AMMONIA; BOX MODELS; DISPERSIONS; ENTHALPY; EXPERIMENTAL DATA; FIELD TESTS; FLOW MODELS; FLUCTUATIONS; GAS FLOW; GAUSS FUNCTION; HEAT TRANSFER; HUMIDITY; INTERPOLATION; JETS; LIQUEFIED GASES; METEOROLOGY; PLUMES; PROBABILITY ESTIMATION; STATISTICS; TEMPERATURE DISTRIBUTION; VELOCITY; WIND

Available on request from:
Information Service Department, Risø National Laboratory
(Afdelingen for Informationsservice, Forskningscenter Risø)
P.O. Box 49, DK–4000 Roskilde, Denmark
Phone (+45) 46 77 46 77, ext. 4004/4005 · Fax (+45) 46 77 40 13
E-mail: infserv@risoe.dk